

# Learning Short Codes for Fading Channels with No or Receiver-Only Channel State Information

Rishabh Sharad Pomaje\* and Rajshekhar V Bhat†

Indian Institute of Technology Dharwad, Dharwad, Karnataka, India

Email: {\*210020036, †rajshekhar.bhat}@iitdh.ac.in

**Abstract**—In next-generation wireless networks, low latency often necessitates short-length codewords that either do not use channel state information (CSI) or rely solely on CSI at the receiver (CSIR). Gaussian codes that achieve capacity for AWGN channels may be unsuitable for *no-CSI* and *CSIR-only* cases. In this work, we design short-length codewords for these cases using an autoencoder architecture. From the designed codes, we observe the following: In the no-CSI case, the learned codes are mutually orthogonal when the distribution of the real and imaginary parts of the fading random variable has support over the entire real line. However, when the support is limited to the non-negative real line, the codes are not mutually orthogonal. For the CSIR-only case, deep learning-based codes designed for AWGN channels perform worse in fading channels with optimal coherent detection compared to codes specifically designed for fading channels with CSIR, where the autoencoder jointly learns encoding, coherent combining, and decoding. In both no-CSI and CSIR-only cases, the codes perform at least as well as or better than classical codes of the same block length.

## I. INTRODUCTION

Modern communication networks transmit information by varying electromagnetic wave characteristics emitted by antennas. These networks are based on electromagnetic theory, information theory, wireless propagation modeling, and antenna theory [1]. With the transition to sixth generation (6G) networks, covering nearly all frequency bands and global environments, integrating these theories is crucial [1], [2]. However, doing so may not yield tractable models for wireless channels which are impaired by time-varying fading. Therefore, it is crucial to develop communication strategies that can operate effectively in fading channels.

For communication over fading channels, techniques like interleaving and diversity using perfect channel state information (CSI) at the receiver (CSIR) and/or transmitter, are first employed to mitigate the effects of fading to make the channel resemble an additive white Gaussian noise (AWGN) channel. Then, codewords designed for AWGN channels are adopted [3]. This is supported by studies such as [4], [5], which suggest that Gaussian codes, capacity-achieving for AWGN channels, also perform well on fading channels asymptotically with infinite interleaving depth and receiver diversity. However, achieving infinite interleaving depth and diversity is impractical due to computational, hardware, and latency constraints. Thus, finite and short blocklength codewords are needed. Designing good short-length codewords is challenging even in AWGN channels, and their performance degradation can be particularly severe in fading environments.

As mentioned in [6], with asymptotic diversity, capacity is achieved in fading channels using Gaussian codebooks and scaled nearest-neighbor decoding. However, capacity is highly sensitive to channel estimation errors, which are particularly challenging to control in dynamic 6G scenarios. Given the overhead associated with channel estimation, communicating without CSI (or with only CSIR) may be more practical, especially in 6G where the number of antennas is large and fading varies rapidly [7]. Various works have explored signal design and capacity derivation for fading channels without CSI. [8] introduces unitary space-time modulation for multiple-antenna links without CSI in Rayleigh block-fading channels, where fading coefficients remain constant over multiple symbol periods. For such channels, [9] derives a capacity expression without CSI, which can be interpreted geometrically as sphere packing in the Grassmann manifold. Moreover, [10], [11] demonstrate that the capacity-achieving distribution for Rayleigh block-fading fading channels without CSI is discrete. Despite these advancements, the development of efficient short-length codewords for Rayleigh and other fading channels under No-CSI and CSIR-Only cases remains a challenging and under-explored area.

Deep learning can be used to design *good* codewords for finite blocklengths in AWGN and fading channels. Previous works [12], [13] show that deep learning-based codewords perform as well as or better than traditional codes in AWGN channels. However, there has been limited exploration of codeword design using deep learning for fading channels, possibly due to the assumption that AWGN-optimized codes would also perform well in fading scenarios, even for finite block lengths. In this work, we assume a fading channel with fixed statistics. Towards addressing the above gaps, our contributions are:

*We design short-length codes specifically for fading channels under no-CSI and CSIR-only cases. In the no-CSI case, we observe that the learned codes are mutually orthogonal when the distribution of the real and imaginary parts of the fading random variable has support over the entire real line,  $\mathbb{R}$ . However, when the support is limited to the non-negative real line,  $\mathbb{R}_+$ , the codes are not mutually orthogonal. For the CSIR-only case, deep learning-based codes designed for AWGN channels perform worse when applied to fading channels with optimal coherent detection compared to codes directly designed for fading channels with CSIR. In the latter case, the deep learning-based autoencoder jointly learns encoding,*

coherent combining, and decoding. In both no-CSI and CSIR-only scenarios, these codes perform at least as well as or better than classical codes of the same block length.

### A. Literature Survey

In [12], an autoencoder with an encoder, noise layer, and decoder is used. The encoder maps message indices to norm-constrained codewords, the noise layer simulates an AWGN channel and the decoder recovers the original message from the noisy codeword. This approach performs comparably to classical codes. Further research has applied similar techniques to degraded broadcast channels [14] and multiple-input multiple-output (MIMO) channels [15].

Deep learning has also been integrated with classical communication systems to enhance receivers [16], [17] and detect sequential codes like convolutional and turbo codes [18]. Additionally, it has been applied to channel estimation in frequency-selective fading channels [19]. In designing communication systems over fading channels, scenarios typically considered include (i) perfect CSI at the receiver (CSIR) but not at the transmitter (CSIT), and (ii) perfect CSIT and CSIR. [15] addresses communication over fading channels with perfect CSIR and CSIT, including scenarios with quantized CSI.

Training an autoencoder end-to-end is challenging without instantaneous channel transfer function knowledge, as the channel must be modeled in intermediate layers, and back-propagation requires functional forms for all layers. Methods to address the above challenge include Simultaneous Perturbation Stochastic Optimization (SPSA) [20] and Generative Adversarial Networks (GANs) [21], where a GAN is trained with encoded signals and pilot data to serve as a surrogate channel for training the transmitter and receiver DNNs.

Following [12], we use an autoencoder to learn short codes for fading channels. However, to the best of our knowledge, none of the above works address the no-CSI and CSIR-only cases in detail, which we focus on.

## II. SYSTEM MODEL AND METHODOLOGY

We consider a point-to-point communication system, where the transmitter communicates information over a wireless fading channel. Specifically, let  $x[l]$  denote the complex symbol transmitted in the  $l$ -th channel use. The receiver observes

$$y[l] = h[l]x[l] + w[l], \quad (1)$$

where,  $w[l]$  represents AWGN with mean 0 and variance  $N_0$ , and  $h[l]$  is the complex channel gain, with variance unity. We assume that  $w[1], w[2], \dots$  are independent and identically distributed (i.i.d.) circularly symmetric complex normal (CSCN) random variables, i.e.,  $w[l] \stackrel{\text{i.i.d.}}{\sim} \text{CSCN}(0, N_0)$ .

We are interested in mapping a message  $m \in \mathcal{M}$ , where  $\mathcal{M}$  represents the set of all possible messages with cardinality,  $|\mathcal{M}| = M$ , to a codeword  $\mathbf{c} = [c_1, \dots, c_n]$ , where  $c_i \in \mathbb{R}$  and  $n$  is the length of the codeword. Each codeword is expected to satisfy an energy constraint:  $\|\mathbf{c}\|_2^2 \leq n$ . Let  $\mathcal{C} = \{\mathbf{c} \mid \mathbf{c} \text{ is a codeword for } m \in \mathcal{M}\}$  be the codebook. The mapping function  $f_\Theta : \mathcal{M} \rightarrow \mathcal{C}$  maps each message

$m \in \mathcal{M}$  to a unique codeword. A codeword  $\mathbf{c}$  is transmitted over a fading channel across consecutive time slots, such that  $x[1] = c_1, x[2] = c_2, \dots, x[n] = c_n$ , after which the next codeword is transmitted. At the receiver, all symbols corresponding to a codeword are collected, resulting in  $\mathbf{y} = [y[1], \dots, y[n]]$ . The goal is to estimate the transmitted message  $m$  using another function,  $g_\Phi : \mathbb{R}^n \rightarrow \mathcal{M}$ . Thus,  $\hat{m} = g_\Phi(\mathbf{y})$  denotes the estimate of the transmitted message. Here,  $\Theta$  and  $\Phi$  are the parameters of the encoding and decoding functions, which we intend to learn. The functions are optimized to minimize the block error rate (BLER), defined as  $\epsilon(M, n) = (1/M) \sum_{m \in \mathcal{M}} \Pr(g_\Phi(\mathbf{y}) \neq m \mid \mathbf{x} = f_\Theta(m))$ , where the relationship between  $\mathbf{y}$  and  $\mathbf{x}$  is given by (1). We empirically compute the BLER as follows:

$$\hat{\epsilon}(M, n) = \frac{1}{N} \sum_{i=1}^N I(m^{(i)}, \hat{m}^{(i)}), \quad (2)$$

where  $I$  is the indicator function defined as  $I(m, \hat{m}) = 0$  if  $m = \hat{m}$ , and  $I(m, \hat{m}) = 1$  otherwise, and  $N$  is the total number of messages sampled uniformly at random from  $\mathcal{M}$ . We denote the BLER as  $\epsilon_{\text{NoCSI}}(M, n)$  and  $\epsilon_{\text{CSIROnly}}(M, n)$  for no-CSI and CSIR-Only cases, respectively.

We denote the energy per coded bit as  $E_b$  and define the signal-to-noise ratio (SNR) as  $\text{SNR}_{\text{linear}} = E_b/N_0$  and  $\text{SNR}_{\text{dB}} = 10 \log_{10} \text{SNR}_{\text{linear}}$ . With  $E_b = 1$ , we adjust the noise variance for different SNRs as follows: For the uncoded case,  $N_0 = 1/(2 \times \text{SNR}_{\text{linear}})$ . For the coded case,  $N_0 = 1/(2 \times R \times \text{SNR}_{\text{linear}})$ , where  $R = \log_2 M/n$ .

We use an autoencoder to learn the functions  $f_\Theta$  and  $g_\Phi$  to minimize (2). The architecture, hyperparameters, models, and source code are available<sup>1</sup>. The autoencoder's input and expected output are one-hot vectors of dimension  $M \times 1$ . Both functions  $f_\Theta$  and  $g_\Phi$  are feedforward neural networks. The encoder's final layer normalizes the output vector to unit norm, which is then scaled by the fading coefficient and perturbed with Gaussian noise. The decoder outputs a probability mass function with  $M$  nodes using a softmax activation function. The loss is the cross-entropy between the one-hot input vector and the decoder's output probabilities.

## III. RESULTS AND DISCUSSION

We now present the results. The energy per codeword is set to  $n$  by design. We adjust the noise variance accordingly to obtain the probability of error versus SNR in the figures.

### A. No CSI Case

We consider both Rayleigh and non-Rayleigh fading cases.

1) *Rayleigh Fading*: We now consider the Rayleigh fading case, where  $h[l] = h_r[l] + jh_i[l] \stackrel{\text{i.i.d.}}{\sim} \text{CSCN}(0, 1)$ . We consider different values of  $M$  with varying  $n$  values. The autoencoder's performance is compared to uncoded orthogonal signaling, mentioned in [22], where the transmitter sends  $[c_1, c_2]$  equal to  $[1, 0]$  and  $[0, 1]$  for bits 0 and 1, respectively. At the decoder, maximum likelihood decoding (MLD) determines

<sup>1</sup>Access the source code here on GitHub.

TABLE I: Codebook learned for  $M = 2$  case for different values of  $n$ . Each element is rounded to two decimal places.

$n$	Codebook
2	[1.41, 0.0], [0.0, -1.41]
3	[0.0, 0.0, -1.73], [1.73, 0.0, 0.0]
4	[0.0, 0.0, 0.0, 1.99], [1.16, -1.17, -1.14, 0.0]
5	[0.0, 0.0, 1.59, 0.0, 1.57], [1.59, 0.0, 0.0, -1.57, 0.0]

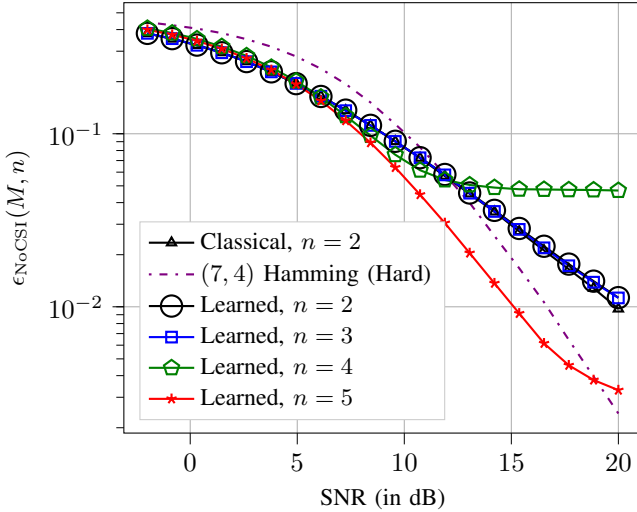


Fig. 1: BLER for  $M = 2$  with varying  $n$ . The training SNR is 7 dB.

bit 0 if  $|y_1| > |y_2|$ , where  $[y_1, y_2]$  is the received vector from these consecutive symbols.

The codewords obtained using the autoencoder and their performance are shown in Table I and Fig.1 for  $M = 2$ , and in Table II and Fig. 2 for  $M = 4$ , respectively. As observed in the tables, the energy per codeword is designed to equal  $n$ , and, importantly, the codewords are mutually orthogonal for each  $n$ . In these figures, for the classical  $n = 2$  case, we use the classical orthogonal signaling mentioned above. For the (7,4) Hamming code, we first encode the bits and then apply orthogonal signaling for transmission, and at the receiver, we first detect the bits using the aforementioned threshold algorithm, which gives hard detection of bits and then proceed with syndrome decoding.

The motivation for exploring different  $M$  and  $n$  stems from the observation that for  $M = 2$  and  $n = 2$ , the autoencoder's performance matched that of classical orthogonal signaling, with the encoder learning the same orthogonal mapping. The decoder, like MLD, compared absolute values. Extending orthogonal signaling to larger  $n$  and  $M$  is non-trivial, but we found that the learned codewords remained orthogonal, with performance improving as  $n$  increased. For  $n = 1$  and  $M = 2$ , it is not possible to find orthogonal codewords with equal energy. In general, no signaling scheme works for  $n < M$ , as we cannot generate more than  $n$  mutually orthogonal vectors in  $n$ -dimensional space.

As expected, when  $M = 2$ , trading off the code rate results in significantly better performance, especially for  $n = 5$ .

TABLE II: Codebook learned for  $M = 4$  case for different values of  $n$ . Each element is rounded to two decimal places.

$n$	Codebook
4	[0.00, 2.0, 0.00, 0.00], [0.00, 0.00, 0.00, -2.0], [2.0, 0.01, 0.01, 0.01], [0.00, 0.00, -2.0, 0.01]
5	[-2.24, 0.0, 0.0, 0.01, 0.0], [0.0, 2.24, 0.0, 0.0, 0.0], [0.02, 0.0, 0.0, 0.01, 2.24], [0.0, 0.0, 0.0, 2.24, 0.0]
6	[0.00, 0.00, 0.00, 0.00, 2.4, 0.00], [0.01, 0.00, 2.4, 0.00, 0.00, 0.00], [2.4, -0.01, 0.00, 0.00, 0.01, 0.00], [0.00, -2.4, 0.0, 0.0, 0.01, 0.00]

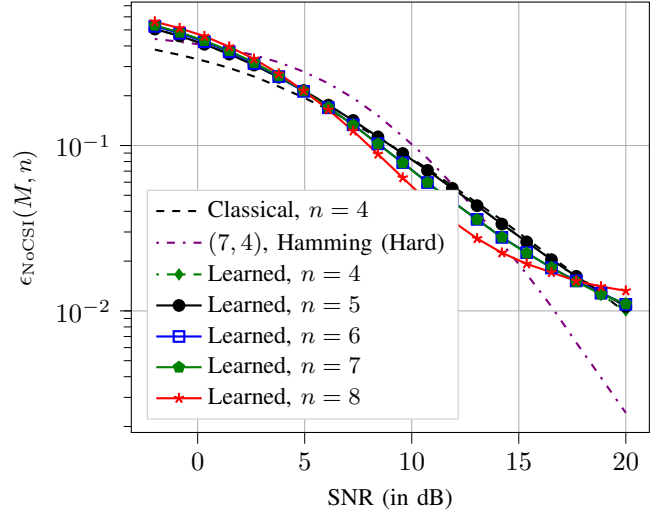


Fig. 2: BLER for  $M = 4$  with varying  $n$ . The training SNR is 10 dB.

This scheme is advantageous for systems or applications prioritizing accuracy over information rate. Additionally, the error rate improvements are most notable in low SNR regions ( $< 10$  dB). However, with  $n = 4$ , a potential issue arises with neural networks. Despite achieving expected training accuracy and loss, the model did not generalize well across a wide range of SNRs during inference. Results for  $M = 4$  is shown in Fig. 2. Increasing the training SNR led to better results. However, the system's generalization to other SNR values is not as good as in the  $M = 2$  case, with autoencoders performing better than conventional methods only in the region around  $10 \pm 5$  dB, where 10 dB is the training SNR.

2) *Non-Rayleigh Fading*: We present the learned codewords and their performance for different distributions on  $h[l] = h_r[l] + jh_i[l]$ , in Table III and Fig. 3, respectively.  $h[l]$  forms a sequence of i.i.d. random variables. We consider cases where  $h_r[l]$  and  $h_i[l]$  are i.i.d. with the following probability density functions (PDF):

- **Distribution I (Rayleigh Fading)**: Normal, with PDF  $f(x; \mu, \sigma^2) = (\sqrt{2\pi\sigma^2})^{-1} e^{-(x-\mu)^2/(2\sigma^2)}$ . The PDF is symmetric around  $x = 0$ .
- **Distribution II**: Custom, with PDF  $f(x; \lambda) = \lambda e^{-\lambda|x|}/2$ . The PDF is symmetric around  $x = 0$ . This distribution was obtained by setting  $X = Y - Z$ , where  $Y, Z \stackrel{i.i.d.}{\sim} \text{Exponential}(\lambda)$ .
- **Distribution III**: Gamma, with PDF  $f(x; k, \theta) = x^{k-1} e^{-x/\theta} (\theta^k \Gamma(k))^{-1}$ . The PDF is asymmetric.

TABLE III: Learned codebook for different distributions of channel fading coefficients in the no-CSI case, with  $M = 2$  and  $n = 2$ . We use the following abbreviations: Symmetric (sym.), Asymmetric (asym.), and Support (supp.).

	Distribution of $h_r$ and $h_l$	Codewords Learned
I.	Rayleigh (sym., supp.: $\mathbb{R}$ )	$[-1.41, 0.0], [0.0, 1.41]$
II.	Custom (sym., supp.: $\mathbb{R}$ )	$[1.41, 0.0], [0.0, 1.41]$
III.	Gamma (asym., supp.: $\mathbb{R}_+$ )	$[1.0, -1.0], [-0.99, 1.0]$
IV.	Gumbel (asym., supp.: $\mathbb{R}$ )	$[-0.0, -1.4], [-1.4, 0.0]$
V.	Folded Normal (asym., supp.: $\mathbb{R}_+$ )	$[-1.0, -0.99], [1.0, 0.99]$

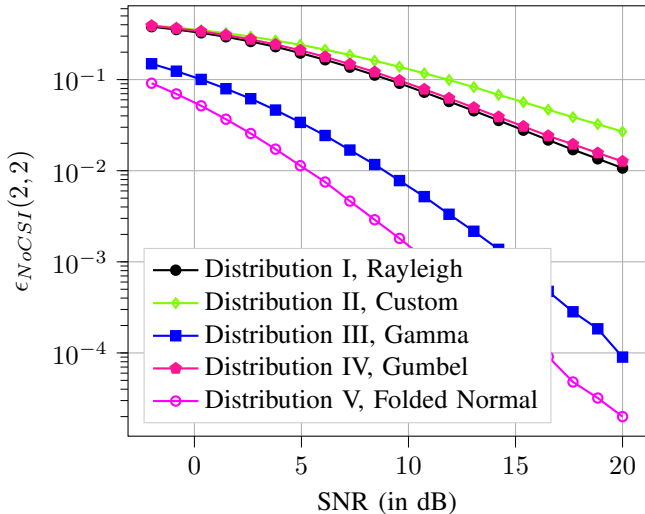


Fig. 3: BLER for  $M = 2$  and  $n = 2$  for different distributions of the channel fading coefficients considered in Table III. The training SNR is 10 dB.

- **Distribution IV:** Gumbel, with PDF  $f(x; \mu, \beta) = \frac{1}{\beta} e^{\left(\frac{x-\mu}{\beta}\right)} - e^{\left(\frac{x-\mu}{\beta}\right)}$ . This PDF is asymmetric.
- **Distribution V:** Folded Normal, with PDF  $f_X(x; \mu, \sigma) = \frac{1}{\sqrt{2\pi\sigma^2}} \left( \exp\left(-\frac{(x-\mu)^2}{2\sigma^2}\right) + \exp\left(-\frac{(x+\mu)^2}{2\sigma^2}\right) \right)$ ,  $x \geq 0$ . To obtain samples from this distribution, we sample normal random variable,  $Y \sim \mathcal{N}(\mu, \sigma^2)$ , and take its absolute value, i.e.,  $X = |Y|$ . This distribution has support  $x \in [0, \infty)$  and is asymmetric.

For a fair comparison, the variances of the fading coefficients under each of the considered distributions are normalized to unity by tuning the distribution parameters accordingly. From Table III, we observe that *the learned codes are mutually orthogonal when the distribution of the real and imaginary parts of the fading random variable, whether symmetric about zero or not, has support over the entire real line,  $\mathbb{R}$ . However, the codes are not mutually orthogonal when the support is the non-negative real line,  $\mathbb{R}_+$* . Further exploration and analysis of this observation will be considered in future work.

### B. CSIR-Only Case

We now consider the CSIR-only case with  $M = 16$  and  $n = 7$ , as shown in Fig. 4. We train the autoencoder at 7 dB SNR for communication over a single-input single-output (SISO) fading channel and compare it with conventional systems: uncoded coherent detection (Uncoded), Hamming (7, 4) hard syndrome decoding with coherent combining ((7, 4) Hamming (Hard)), and Hamming (7, 4) soft decoding with

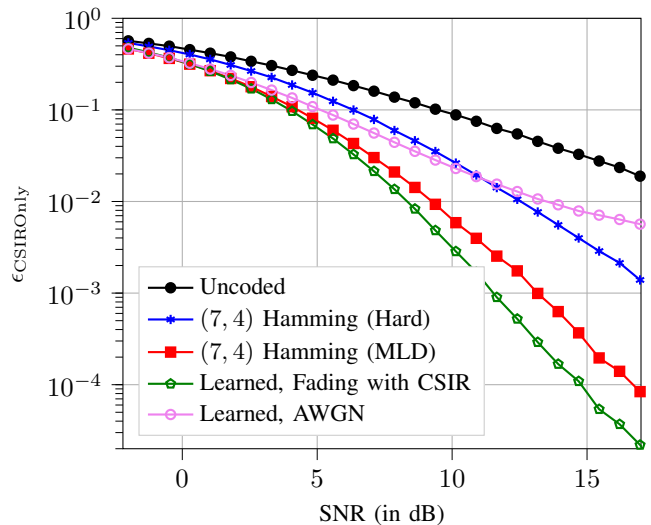


Fig. 4: BLER for  $M = 4$  with  $n = 7$ . The training SNR is 7 dB. The fading channel considered is a single-input single-output channel.

maximum-likelihood decoding and coherent combining ((7, 4) Hamming (MLD)). From the figure, we observe that the autoencoder-based code performs comparably to the (7, 4) Hamming (MLD), which is the best-performing benchmark, at lower SNRs and outperforms it at higher SNRs.

To demonstrate the optimization of learned codewords, we first trained an autoencoder for an AWGN channel. We then applied these codes to a fading channel by using the encoder to encode the bits, which are passed through the fading channel. At the receiver, we manually perform coherent combining before inputting the signal to the decoder. The results, as shown by the (Learned, AWGN) curve, indicate poor performance in the fading channel.

## IV. CONCLUSION AND FUTURE RESEARCH

We obtained short-length codewords using a deep learning autoencoder-based approach for both no-CSI and CSIR-only cases. In the no-CSI case, with  $M = 2$  and  $n = 2$ , the autoencoder learned orthogonal signaling similar to classical techniques under Rayleigh fading. Further exploration with different  $M$  and  $n$ , and distributions showed that the learned codes are mutually orthogonal when the distribution of the real and imaginary parts of the fading random variable has support over the entire real line,  $\mathbb{R}$ . However, when the support is limited to the non-negative real line,  $\mathbb{R}_+$ , the codes are not mutually orthogonal. For the CSIR-only case, codes designed for AWGN channels performed worse in fading channels with optimal coherent detection compared to codes specifically designed for fading channels with CSIR, where the autoencoder jointly learns encoding, coherent combining, and decoding. In both no-CSI and CSIR-only scenarios, these codes perform as well as or better than classical codes of the same block length. Future work includes learning codebooks for MIMO channels with various channel fading distributions and for multi-user communication scenarios.

## REFERENCES

- [1] C.-X. Wang *et al.*, “Electromagnetic Information Theory: Fundamentals and Applications for 6G Wireless Communication Systems,” *IEEE Wireless Commun.*, pp. 1–8, 2024.
- [2] M. Z. Chowdhury, M. Shahjalal, S. Ahmed, and Y. M. Jang, “6G Wireless Communication Systems: Applications, Requirements, Technologies, Challenges, and Research Directions,” *IEEE Open J. Commun. Soc.*, vol. 1, pp. 957–975, 2020.
- [3] E. Biglieri, G. Caire, and G. Taricco, “Coding for the fading channel: a survey,” *Signal Processing*, vol. 80, no. 7, pp. 1135–1148, 2000.
- [4] J. Ventura-Traveset, G. Caire, E. Biglieri, and G. Taricco, “Impact of diversity reception on fading channels with coded modulation. I. Coherent detection,” *IEEE Trans. Commun.*, vol. 45, no. 5, pp. 563–572, 1997.
- [5] G. Wornell, “Spread-response precoding for communication over fading channels,” *IEEE Trans. Inf. Theory*, vol. 42, no. 2, pp. 488–501, 1996.
- [6] A. Lapidoth and S. Shamai, “Fading channels: how perfect need “perfect side information” be?” *IEEE Trans. Inf. Theory*, vol. 48, no. 5, pp. 1118–1134, 2002.
- [7] X. Yang, “Capacity of fading channels without channel side information,” 2019. [Online]. Available: <https://arxiv.org/abs/1903.12360>
- [8] B. Hochwald and T. Marzetta, “Unitary space-time modulation for multiple-antenna communications in Rayleigh flat fading,” *IEEE Trans. Inf. Theory*, vol. 46, no. 2, pp. 543–564, 2000.
- [9] L. Zheng and D. Tse, “Communication on the Grassmann manifold: a geometric approach to the noncoherent multiple-antenna channel,” *IEEE Trans. Inf. Theory*, vol. 48, no. 2, pp. 359–383, 2002.
- [10] I. Abou-Faycal, M. Trott, and S. Shamai, “The capacity of discrete-time memoryless Rayleigh-fading channels,” *IEEE Trans. Inf. Theory*, vol. 47, no. 4, pp. 1290–1301, 2001.
- [11] M. Chowdhury and A. Goldsmith, “Capacity of block Rayleigh fading channels without CSI,” in *IEEE ISIT*, 2016, pp. 1884–1888.
- [12] T. O’Shea and J. Hoydis, “An Introduction to Deep Learning for the Physical Layer,” *IEEE Trans. Cogn. Commun. Netw.*, vol. 3, no. 4, pp. 563–575, 2017.
- [13] T. Erpek, T. J. O’Shea, Y. E. Sagduyu, Y. Shi, and T. C. Clancy, “Deep Learning for Wireless Communications,” 2020.
- [14] E. Stauffer, A. Wang, and N. Jindal, “Deep Learning for the Degraded Broadcast Channel,” in *Asilomar Conference on Signals, Systems, and Computers*, 2019, pp. 1760–1763.
- [15] T. J. O’Shea, T. Erpek, and T. C. Clancy, “Deep Learning Based MIMO Communications,” 2017.
- [16] D. Neumann, T. Wiese, and W. Utschick, “Learning the MMSE Channel Estimator,” *IEEE Trans. Sig. Proc.*, vol. 66, no. 11, pp. 2905–2917, 2018.
- [17] N. Farsad and A. Goldsmith, “Neural Network Detection of Data Sequences in Communication Systems,” *IEEE Trans. Sig. Proc.*, vol. 66, no. 21, pp. 5663–5678, 2018.
- [18] H. Kim, S. Oh, and P. Viswanath, “Physical Layer Communication via Deep Learning,” *IEEE J. Sel. Areas Inf. Theory*, vol. 1, no. 1, pp. 5–18, 2020.
- [19] H. Ye, G. Y. Li, and B.-H. Juang, “Power of Deep Learning for Channel Estimation and Signal Detection in OFDM Systems,” *IEEE Wirel. Commun. Lett.*, vol. 7, no. 1, pp. 114–117, 2018.
- [20] V. Raj and S. Kalyani, “Backpropagating Through the Air: Deep Learning at Physical Layer Without Channel Models,” *IEEE Commun. Lett.*, vol. 22, no. 11, pp. 2278–2281, 2018.
- [21] H. Ye, L. Liang, G. Y. Li, and B.-H. Juang, “Deep Learning-Based End-to-End Wireless Communication Systems With Conditional GANs as Unknown Channels,” *IEEE Trans. Wirel. Commun.*, vol. 19, no. 5, pp. 3133–3143, 2020.
- [22] D. Tse and P. Viswanath, *Fundamentals of Wireless Communication*. Cambridge University Press, 2005.